Ultraviolet control of bacterial biofilms in microfluidic chips

Gabriel Ramos, Clara Toulouze, Maya Rima, Olivier Liot, Paul Duru, Yohan Davit

▶ **To cite this version:**

Gabriel Ramos, Clara Toulouze, Maya Rima, Olivier Liot, Paul Duru, et al.. Ultraviolet control of bacterial biofilms in microfluidic chips. Biomicrofluidics, 2023, 17 (2), pp.024107. 10.1063/5.0135722 . hal-04191274

HAL Id: hal-04191274
https://hal.science/hal-04191274v1

Submitted on 30 Aug 2023

HAL is a multi-disciplinary open access archive for the deposit and dissemination of scientific research documents, whether they are published or not. The documents may come from teaching and research institutions in France or abroad, or from public or private research centers.

L'archive ouverte pluridisciplinaire **HAL**, est destinée au dépôt et à la diffusion de documents scientifiques de niveau recherche, publiés ou non, émanant des établissements d'enseignement et de recherche français ou étrangers, des laboratoires publics ou privés.

Ultraviolet control of bacterial biofilms in microfluidic chips

Gabriel Ramos[a], Clara Toulouze[a], Maya Rima[b], Olivier Liot[a], Paul Duru[a] and Yohan Davit[a*]

[a] *Institut de Mécanique des Fluides (IMFT), CNRS & Université de Toulouse, 31400 Toulouse, France*

[b] *Laboratoire de Génie Chimique (LGC), Université de Toulouse, CNRS, INPT, UPS, 31062 Toulouse, France*

Abstract

PDMS microfluidic systems have been instrumental in better understanding couplings between physical mechanisms and bacterial biofilm processes, such as hydrodynamic effects. However, precise control of the growth conditions, for example the initial distribution of cells on the substrate or the boundary conditions in a flow system, has remained challenging. Furthermore, undesired bacterial colonization in crucial part of the systems, in particular in mixing zones or tubing, are an important factor that strongly limits the duration of the experiments and therefore impedes our ability to study the biophysics of biofilm evolving over long periods of time, as found in the environment, in engineering or in medicine. Here, we develop a new approach that uses ultraviolet-C (UV-C) light emitting diodes (LEDs) to confine bacterial development to specific zones of interest in the flow channels. The LEDs are integrated into a 3D printed light guide that is positioned upon the chip and used to irradiate germicidal UV-C directly through the PDMS. We first demonstrate that this system is successful in controlling undesired growth of *Pseudomonas aeruginosa* biofilm in inlet and outlet mixing zones during 48 hours. We further illustrate how this can be used to define the initial distribution of bacteria, to perturb already formed biofilms during an experiment and to control colonization for seven days — and possibly longer periods of time — therefore opening the way towards long-term biofilm experiments in microfluidic devices. Our approach is easily generalizable to existing devices at low cost and may thus become a standard in biofilm experiments in PDMS microfluidics.

1 Introduction

Bacteria primarily live within biofilms — communities of microorganisms adherent to an interface and embedded in a self-produced matrix of extracellular polymeric substances [1, 2, 3, 4, 5]. Biofilms are ubiquitous on Earth [6, 7] and have a considerable impact on human health, natural environments and industrial processes [2, 8]. They play an important role in various pathologies, including cystic fibrosis and chronic wounds [9, 10]. They drive fundamental biogeochemical processes, such as carbon [11] or nitrogen [12] cycles. They are also key in water processing and engineering applications, for example in biofiltration [13] or bioremediation [14].

The behavior of a biofilm is complex and differs significantly from that of individual microorganisms that constitute it. Biofilm exhibit 'emergent properties' [1], such as enhanced resistance to antibiotics, biocides and predators compared to free-floating planktonic bacteria. The large density of different microorganisms present in biofilms is also favorable to social interactions [4], which can lead to the emergence of complex spatiogenetic patterning [15]. Furthermore, biofilms are heterogeneous systems undergoing a variety of gradients [16], such as pH [17], nutrients [18] and oxygen [19]. Understanding the complexity of biofilms and the many cues that drive their behavior is an open challenge overlapping biophysics, microbiology and ecology.

Microfluidic approaches have proven to be a powerful tool in studying bacteria and biofilms (see discussion in [20]). PDMS micropatterning and microfluidics [21], in particular, provide the ability to precisely control the condition of development and to isolate the role of a specific phenomenon. PDMS has many advantages in microfluidic applications [22]. It has excellent optical properties, is cheap, stable, non-toxic and permeable to oxygen [23, 24]. This has made PDMS micropatterning the most widely used microfluidic tool to studying biological systems [21]. Such technologies have brought new insight into a broad range of phenomena [25] including interactions of bacteria with flow [2, 5], the effect of gradients, motility and taxis [26], communications [27] and the dynamics of social interac-

* Corresponding author: yohan.davit@imft.fr

tions [28].

We argue that one of the limitations of current PDMS systems is their inability to confine the biofilm to a zone of interest. Over time, motile bacteria will colonize all parts of the system and form biofilm in the nutrient supplies, the tubing, the pumps and the sensors. This has important consequences on the experiments. It may affect the quality and interpretation of the results, making it particularly difficult to control boundary conditions — e.g. how much nutrient is at the inlet if there is biofilm in the tubing? It also limits biofilm experiments to short timescales, with most experiments in microfluidic systems focusing on the early stages of biofilm development, often over a few hours [29, 27, 5], very rarely over two or three days [30, 31]. In contrast, biofilms in medical, environmental or industrial conditions evolve over days, weeks, months or even years. This makes it necessary to develop technologies to study them in laboratory-controlled conditions over long time scales.

Here, we develop a novel low-cost approach that allows us to confine biofilm growth to specific zones in the flow channels. We present a device consisting of ultraviolet-C (UV-C) light-emitting diodes (LEDs) integrated into a 3D printed light guide that is used to irradiate germicidal UV-C through the PDMS and confine bacterial development to specific zones of interest. Our experimental setup is detailed in section 2 along with the material and methods used throughout the paper. To test the effectiveness of our approach, we present in Section 3 an application to a model system where *Pseudomonas aeruginosa* biofilms are grown in a network of flow channels. We also show that the same UV-C irradiation approach through the PDMS can be used to define initial conditions and generate perturbations of biofilm processes.

2 Experimental setup

2.1 PDMS chip

We used photolithography methods for the mold fabrication using dry film negative photoresist (EMS-Nagase DF10100) on a silicon wafer. The device was made using polydimethylsiloxane (PDMS, Sylgard 184) with a reticulant agent in a ratio 1:10 and the chip was bonded to a glass slide by means of a corona plasma wand (Electro-Technic BD-20AC Corona surface treater). The microfluidic chip consists of two mixing zones and a honeycomb channel network (Fig 1B), with each channel having a cross section of 100 μm x 100 μm. Before bacterial inoculation, the microfluidic device is degassed inside the desiccator for 1 h, the channels are cleaned using ethanol, and finally the

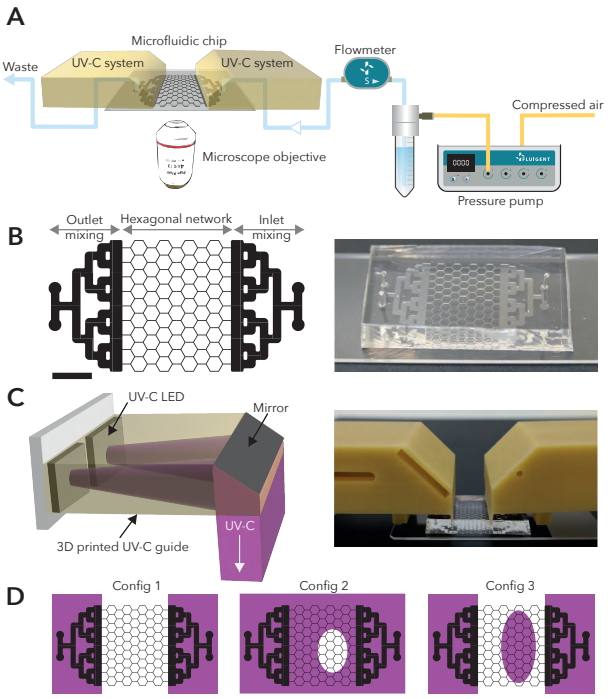

Figure 1 Experimental setup. **A.** Schematics of the fluidic system. A constant flowrate is imposed through the microfluidic chip using a pressure pump coupled with a flow meter. Image acquisition is performed every hour with an inverted microscope using a 4x objective. Two UV-C systems irradiate both the inlet and outlet of the chip during the total duration of the experiment. **B.** Microfluidic chip. On the left, the schematic shows the different regions: the mixing zones (inlet and outlet) and the hexagonal network channels. On the right, we present a picture of the micro-patterned PDMS plasma bonded directly to a glass slide. Scale bar is 5 mm. **C.** UV-C device. The schematic on the left shows a pair of UV-C LEDs attached to a 3D printed guide with a mirror on its edge that reflects the UV-C light onto the desired zones. On the right, an actual image of the positioning of the UV-C system is presented. **D.** Irradiated zones on the chip (purple zones) for three different UV-C configurations used in the experiments. No network irradiation (Config 1), control of initial conditions (Config 2), and perturbation on the network (Config 3). In Config 2, a small aluminum cylinder blocks the light to protect part of the network exposed to a central UV-C LED, while in Config 3 an aluminum plate with a hole in its center allows the irradiation of a portion of the network. The resulting patterns are not circular in the protected zone in Config 2 and in the irradiated zone in Config 3 because the angle of incidence of the central UV-C light was slightly deviated from the normal to the PDMS surface.

device is filled with fresh culture medium.

2.2 Culture of bacteria and inoculation of the chip

We use *Pseudomonas aeruginosa* strain ATCC 15692 GFP. The strain is collected from a -80°C stock and cultured overnight in 10 mL of Brain Heart Infusion (BHI, Merck, 37.5 g/L) with ampicillin (300 μg/mL) at 30°C and 180 RPM. The next day, part of the culture is diluted to obtain an optical density at 600 nm (OD_{600}) of 0.7. This concentration ensures bacterial attachment during the inoculation phase. Inoculation is performed flowing simultaneously culture medium and ~100 μL of bacterial suspension using two inlets, each one at 8 μL/min. After inoculation, the bacterial inlet is sealed with silicone to avoid colonization by remaining bacteria, while the culture medium inlet continues flowing without detaching the initially adhered bacteria (see SI). Then, the flow rate is set to 2 μl/min for the rest of the experiment.

2.3 Flow system

Flow rate is imposed using a pressure pump (Fluigent MFCS-EZ) coupled to a flow meter (Fluigent Flow Unit S). Both the pump and the flow meter are connected to a computer and controlled by a software (Fluigent A-i-O) that continuously adapt the pressure values in order to impose a constant flow rate (Fig 1A). The culture medium flowing during the whole experiment is BHI with ampicillin (300 μg/mL) containing red passive tracers (Invitrogen FluoSpheres carboxylate 1.0 μm red 580/605) suspended in a concentration of 6.7 μg/mL. Spheres can attach to the biofilm without significantly modifying colonization of the network (see the Supplementary infomation). The temperature of the device and the culture medium is maintained at 30°C using a cage incubator (Okolab).

2.4 Imaging

The microfluidic device is imaged using an inverted microscope (Nikon Eclipse Ti2-E) with a 4x objective (Plan Fluor 0.13 NA) and imaged using a sCMOS camera (PCOedge 4.2bi). Timelapse microscopy is performed by taking images automatically every hour using the JOBSÂ® module from NIS-Elements AR. Images are taken in bright field (BF, 30 ms exposure time) and in green fluorescence (GFP, 80 ms exposure time). For fluorescence images, a light source (Lumencor Sola light engine SM at 10%) filtered by a cube (Nikon filter cube GFP-3035D) excites the green fluorescence protein produced by the bacteria (GFPmut3).

In order to observe the fluid flow paths complementary to direct biofilm imaging, Particle Tracking Velocimetry (PTV) is performed using the red passive fluorescent tracers suspended in the culture medium and recorded using a fast camera (PCO Dimax) during 170 ms at 100 fps and 2 ms exposure time. The Sola light source for fluorescence was at 100% to improve the image contrast due to the high speed of the particles, and a cube (MXR00708 TRITC-B 32 mm) filtered the light to excite the tracers.

Both biofilm images and PTV videos are performed in mosaic, scanning 30 positions to reconstruct the final image. The total scanning time is of the order of seconds, while the typical doubling time of bacteria in rich medium is between 25 and 35 min [32] and hence, there are no changes of the global state of the chip between the first and the last image of the mosaic.

2.5 UV-C irradiation device for inlet and outlet

Two UV-C LED sources (CHTPON 1 W-20 mm-120Â°) irradiating at 275 nm are attached to a 3D printed piece containing a special UV mirror (Edmund Optics TECHSPECÂ® 20x20 mm^2) in order to constantly expose the mixing zones of the device to UV-C light (Fig 1C and purple areas in Fig 1D). Intensity of UV-C LEDs is regulated by a homemade electronic controller connected to a computer. In situ measurements of the irradiance were performed on every mixing zone using a photo/radiometer (Delta Ohm Portable Luxmeter HD 2102.1) connected to an UV-C probe (Delta Ohm LP471UVC irradiance probe). The transmittance we measured through a 4 mm PDMS layer is about 54%, yielding an irradiance of ~9.3 $\mu W/cm^2$ on the mixing zone. Considering that an element of fluid takes ~172.5 s to go through the mixing zone at the flow rate studied in this article (2 μL/min), we estimate that the dose received by the culture media before being consumed by bacteria is ~1.6 mJ/cm^2. We performed experiments at different doses to test the impact of UV-C on culture media (0, 12.9 and 129 mJ/cm^2), and we did not observe any significant influence on the viability of cell culture. For more details, see the Supplementary information.

2.6 UV-C irradiation for initial condition and perturbations

A third UV-C source irradiating at 265 nm is directly placed above the microfluidic device (Klaran, 70 mW KL265-50V-SM-WD) to control initial conditions and perform perturbations on the system (Configs 2 and 3 in Fig 1D). In both cases the LED is irradiating at 138 $\mu W/cm^2$. To control initial conditions, the central UV-C LED is on for 20 hours from the beginning of the experiment and then is removed. In order to protect a portion of the network from UV-C

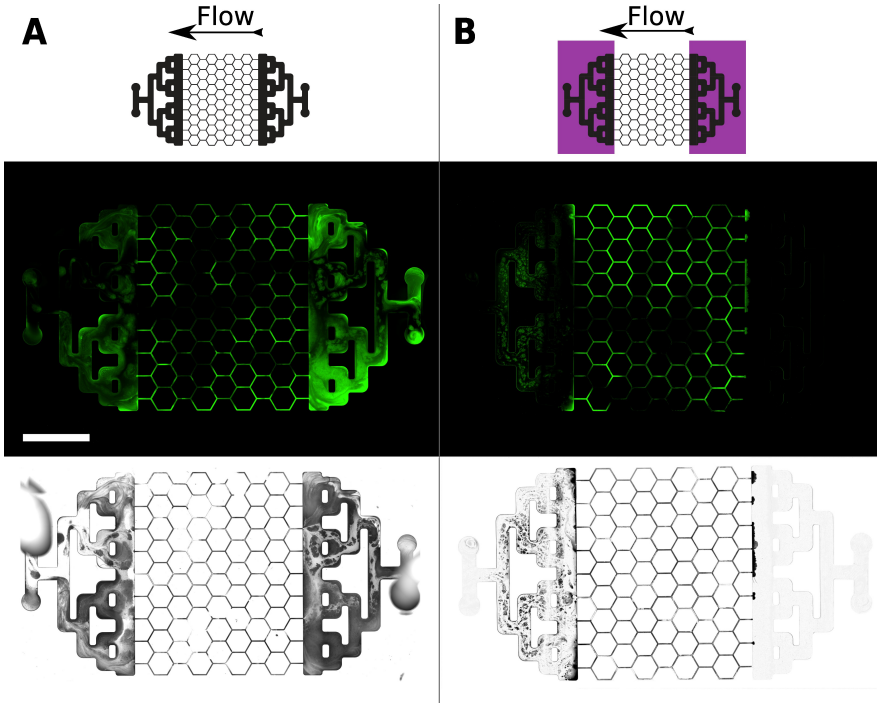

Figure 2 UV-C can be used to prevent inlet colonization and to limit outlet biofilm attachment. The schematics show the area irradiated by the UV-C LEDs (purple color) with arrows indicating the direction of the flow. Fluorescence images are on the top (black and green) and bright field images (gray levels) on the bottom. **A.** Fully developed biofilm after 48 h without UV-C. Brighter green regions in fluorescence and darker regions in bright field indicate biofilms. Without UV-C, the biofilm is fully colonizing the mixing zones at both the inlet and outlet. **B.** Fully developed biofilm after 48 h using UV-C LEDs. The inlet is clean and the biofilm on the outlet, which comes from detachments within the network, is limited by the UV-C irradiation. Both experiments were performed at 2 μL/min at 30°C. The scale bar is 5 mm.

radiation, an aluminum-made obstacle is placed onto the microfluidic device (Fig 1D Config 2). To perform perturbations, the central UV-C LED is turned on after 14 hours of biofilm development. The irradiation is performed during 24 hours and then the UV-C LED was removed to let the biofilm develop again. To define the region to be perturbed, an aluminum-made plate with a hole in its center is placed onto the microfluidic device (Fig 1D Config 3).

2.7 Image processing

Fluorescence images were treated using Fiji [33] to subtract the background and adjust the contrast for biofilm visualization. Bright field images were processed with homemade Matlab scripts for increasing the image intensity of the mixing zones, which received less illumination due to the presence of the UV-C system, and for improving the contrast between the background and the channels by the application of a mask on the image. PTV images were treated by subtracting the background and then detecting particles using a custom Python script. The reconstruction of trajectories were perfomed in Matlab using an optimization algorithm (Hungarian algorithm). Resulting PTV images were created with homemade scripts in Matlab, overlaying the detected particle tracks with the average image of the video. The relative intensity of GFP fluorescence was computed by adding pixel intensities over either the inlet or outlet mixing zones after noise filtering and normalization by the maximum pixel intensity found on the image sequence.

3 Results and discussion

3.1 UV-C irradiation prevents colonization of the mixing zones

We first aim at validating our approach by comparing biofilm growth in microfluidic chips with (Config 1) and without using our device to irradiate UV-C in the inlet and outlet mixing zones. Experiments consisted in inoculating GFP-tagged *P. aeruginosa* in the channels, then flowing the culture medium at 2 μL/min to let the biofilm grow and visualizing growth through time-lapse fluorescence and bright field microscopy. In the case with UV-C, the illumination of the inlet and outlet mixing zones is constant throughout the experiment. Fig 2 shows images after 48 h of growth with flow from right to left and Fig 3 the integrated fluorescence intensity over inlet and outlet mixing zones after 42 h for triplicates. In the inlet mixing zone, we see that the chip without UV-C has a large

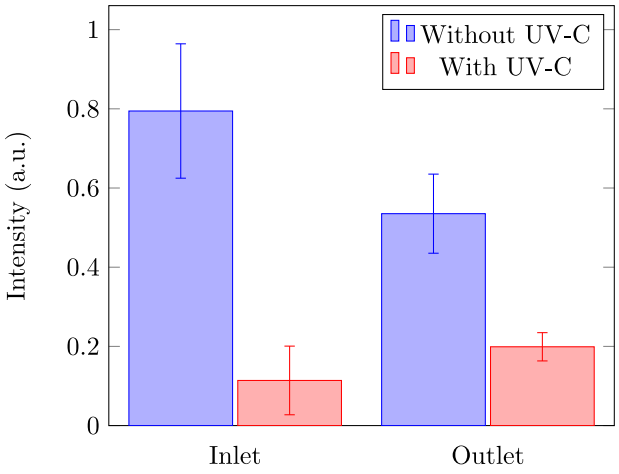

Figure 3 Relative intensity of GFP fluorescence in arbitrary unit (a.u.) integrated over the inlet and outlet mixing zones with and without UV-C irradiation after 42 hours at 2 μL/min and 30°C. The histogram shows the average values of triplicates with standard error. Without UV-C the values are 0.80±0.17 (Inlet) and 0.54 ± 0.10 (Outlet). With UV-C the values are 0.11 ± 0.09 (Inlet) and 0.20 ± 0.04 (Outlet)..

quantity of biomass (mean intensity 0.80 a.u. in Fig 3 after 42 h) with visible streamers (i.e. filamentous biofilm structures following the flow) and channels that seem entirely clogged. Biofilm was also visible to the naked eye in the inlet tubing, showing that motile bacteria had traveled against the flow for colonization. On the contrary, in the chip with UV-C, the inlet mixing zone is almost completely clean (mean intensity 0.11 a.u. in Fig 3 after 42 h). UV-C irradiation inactivates free-floating and initially attached bacterial cells by interfering with transcription and replication [34]. Biofilm only managed to slightly grow against the flow from the first channels of the hexagonal network and appear as small mushroom-like structures. These structures seemed to "burst" upon reaching the zone with strong UV illumination (see supplementary Movie 1). No biofilm was visible in the inlet tubing.

For the outlet, we again observe that a large quantity of biomass has formed in the case without UV-C (mean intensity 0.54 a.u. in Fig 3 after 42 h). In the case with UV-C, biofilm managed to attach to the PDMS and glass, which was not the case for the inlet. However, the quantity of biofilm is smaller than in the case without UV-C, thus showing that the irradiation is efficient in controlling the formation of biofilms but cannot prevent it completely (mean intensity 0.20 a.u. in Fig 3 after 42 h). It has been previously

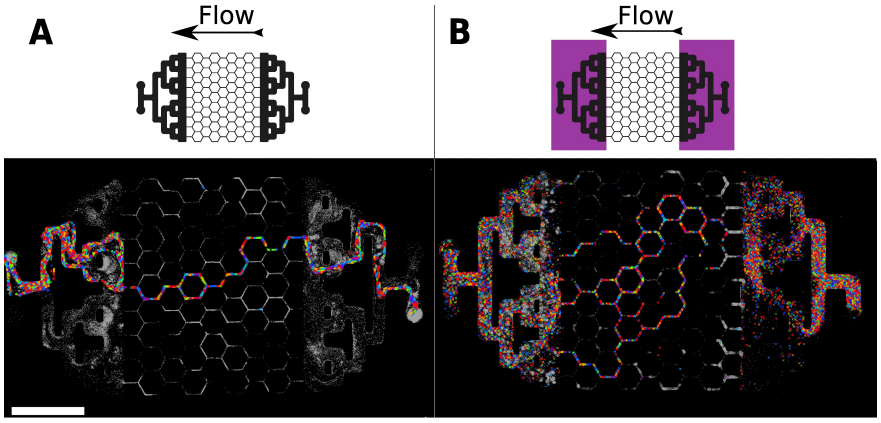

Figure 4 UV-C can be used to control boundary conditions. Using particle tracking velocimetry (PTV), we observe the flow paths through the microfluidic system. Each color represents a detected trajectory of one tracer particle. **A.** Experiment without UV-C. The biofilm developed in the mixing zones drives the flow through the network with a single channel. **B.** Experiment with UV-C. Clogging in the mixing zones is negligible and flow is controlled by hydraulic conductivities in the hexagonal network. Both experiments show the biofilm formation 48 h after the inoculation at 30°C and 2 μL/min. Scale bar 5 mm.

shown that the biofilm matrix can act as a shield to UV-C irradiation [35, 36]. Since we observed regular detachment of large patches of biofilm from the hexagonal network, we hypothesize that bacteria visible at the outlet are much more resilient to UV-C because they initially formed in the network and then got transported in the mixing zone. This was not observed in the inlet because bacteria are either initially present from the inoculation or move to this zone using their bulk or surface motility. Therefore, bacteria at the inlet are irradiated in their planktonic state and never have the opportunity to form a biofilm that would shield them from part of the UV-C.

3.2 UV-C irradiation control boundary conditions

To further assess the effect of the UV-C, we now study the impact of biofilm colonization in the mixing zones on the flow. We want to determine whether flow in the zone of interest is perturbed by biomass forming in the mixing zones and whether UV-C irradiation can modify flow boundary conditions. The idea is that the pressure distribution at the inlet and outlet of the network should be approximately uniform. The flow, on the other hand, should be controlled by the distribution of hydraulic conductivities in the network, which locally scales with the channel hydraulic radius as ${r_h}^4$, and thus strongly depends on the amount of biofilm in each branch.

Figure 4 compares the trajectories of fluorescent microparticles with and without UV-C. In the case without UV-C, particles are localized in specific zones of the system and only a single flow channel has formed through the structure. This is a common trend observed when the inlet mixing zone is colonized (see supplementary information section 6). We hypothesize that the unwanted clogging is such that the conductivity of channels in the mixing zones is driving the flow, not growth in the hexagonal network. In the case with UV-C, particles have been transported almost everywhere in both mixing zones and several flow channels have formed through the zone of interest. This suggests that UV-C is efficient in controlling boundary conditions of the zone of interest.

Beyond flow, the presence of a large quantity of biomass in the inlet mixing zone and in the tubing is also expected to strongly modify mass transport and induce, in particular, uncontrolled nutrient uptake before the network. This would lead to difficulties in the interpretation of the results with most nutrients being consumed before reaching the hexagonal network. In that sense,, we see that we will have a much more homogeneous condition in the case with UV-C.

3.3 UV-C irradiation can be used to control initial conditions

The optical approach to controlling the spatial distribution of the biomass can be used for other purposes and we provide example applications in the following sections. As an illustration, we show here that we can initially localize bacteria to a specific portion of the zone of interest.

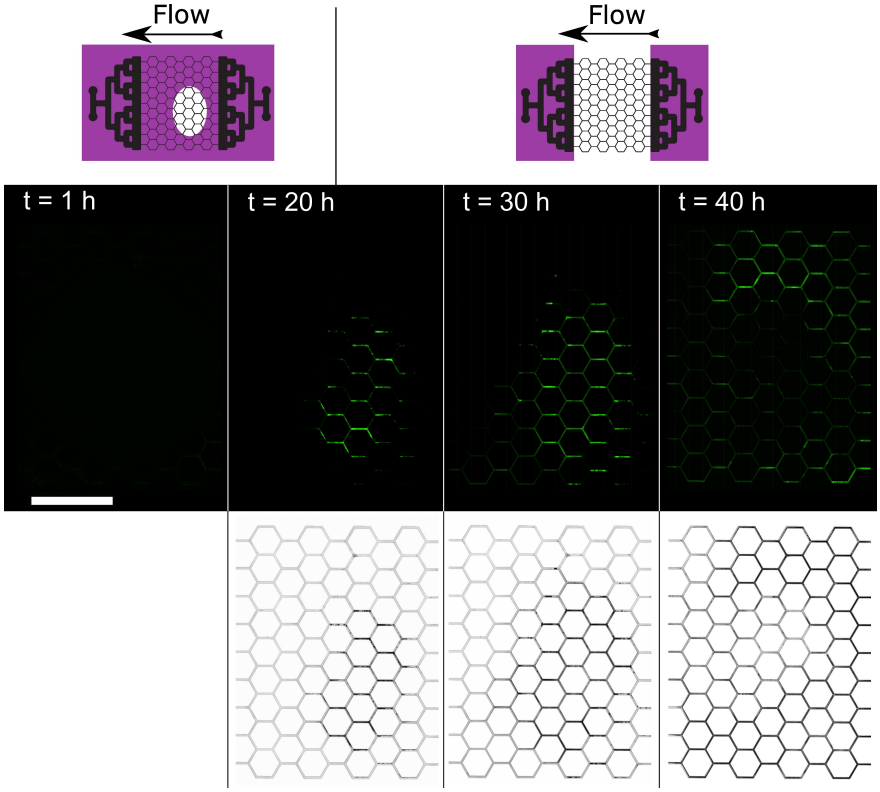

Figure 5 UV-C can be used to control bacterial localization at initial times. The drawing shows the area irradiated by the UV-C led (purple color), the top row shows the images in fluorescence and the bottom row the images in bright field. The first bright field image is missing, because the UV-C LED above the device is blocking the white light from the microscope. The central UV-C LED was operational above the device for 20 h after inoculation, and then was removed. During this first stage of the experiment, UV-C irradiation prevented biofilm formation everywhere except in the protected region (bright green zones in fluorescence and dark zones in bright field). After UV-C removal, from 20 h to 40 h, the biofilm starts expanding and colonizes the rest of the device. The experiment was performed at 30°C and 2 μL/min. Scale bar 5 mm.

To do so, we performed the same inoculation procedure, but then illuminated the hexagonal network with a separate UV-C LED, using a mask to shield part of the illumination. The idea was that we should have active bacteria only in the zone that was protected from UV-C and thus that we can define the initial boundary of the growth problem. Fig 5 shows the timelapse images in green fluorescence and bright field after 1, 20, 30 and 40 hours of growth. We indeed see that biofilm initially forms in the zone shielded from UV-C. The mechanism here is the same as in the inlet (see Section 2). Bacteria damaged by the UV-C are evacuated from the channels with the flow, while cells that were shielded are able to form biofilms. We then observe a second phase with a more complex dynamics at about 40 h, when bacteria have had time to colonize the rest of the system and biofilm has started forming everywhere in the network.

3.4 UV-C irradiation can be used to induce perturbations

We further wanted to determine whether UV-C could be used to perturb an already formed biofilm, which is a much more difficult problem than just changing the initial conditions. In the case of the initial conditions, only individual bacteria or small microcolonies had formed in the network and we have seen in section 3.1 that the efficiency of the UV-C treatment depends upon the maturity of the biofilm. Here, we proceeded to growing biofilm in the zone of interest without any UV-C for 14 h and then illuminating this zone with UV-C for 24 h (Fig 6). We observed important changes in the spatial distribution of the biofilm through the network with a significant decrease of the total biomass. Upon stopping the UV-C and letting growth continue, we also recovered biofilm everywhere in the system with a distribution reminiscent to that after 14 h.

3.5 UV-C irradiation makes week-long experiments possible

One of the main goals of this paper was to determine whether the UV-C illumination could be used to perform longer term biofilm experiments in microfluidic systems. To test this, we reproduced the experiment in Fig 2 twice over both 5 days and an entire week. For the week-long experiment, results in Figs 7 and 8 show that the colonization of mixing zones after 1 week is similar to that after 3 days, with almost no biomass in the inlet mixing zone and little biofilm in the outlet. In the case of the 5 days experiment, the UV-C system was not perfectly aligned with the boundary of the hexagonal network. It thus allowed biofilm to grow from the network into the mixing zones forming a layer of biofilm on the boundary (section 7 in the supplementary material), with a significant impact upon the results. Even though the time-lapse imaging still shows that colonization remains controlled in the rest of the mixing zones, this case shows that the UV-C system should be positioned carefully.

4 Conclusions and outlook

Ultraviolet-C, particularly in the range 250 to 270 nm, have long been known to damage the genetic material of microorganism and thus to be germicidal [34]. The advent of UV-C light-emitting diodes [37, 38] has made it possible to develop new approaches to mitigating microorganisms growth, for instance in water resources management [39, 40]. In this paper, we have shown that UV-C LEDs combined with masks and simple light guides can be used to delineate bacterial growth to a specific zone of interest in microfluidic channels. Our approach takes advantage of the transparency of PDMS to UV-C to illuminate specific zones of the system directly through the PDMS. We have used this approach to eliminate bacterial growth outside the area of interest in the flow system and to control initial and boundary conditions of the zone of interest. Further, we have also shown that this allows us to perform microfluidic experiments without colonization of the tubing or mixing zones for 7 days. When the UV-C system was positioned properly, the state of the colonization after 3 or 7 days was similar, thus suggesting that experiments could be run for an even longer period of time, possibly several weeks. This may open the way towards long-term biofilm experiments in microfluidic devices.

One limitation is the ability to prevent growth and attachment of already formed biofilms. Extracellular polymeric substances partly protect bacteria from UV-C so that some biofilm pre-formed in the hexagonal network was able to subsist in the outlet. However, our system was able to efficiently prevent further growth and thus control the impact on the flow. For *P. aeruginosa,* a dose of 4 mJ/cm^2 is enough for a 2 log inactivation [40]. Since our irradiance in the mixing zones was about 9.3 μW/cm^2, a 2 log inactivation is thus expected in about 7 minutes. However, the same dose is less efficient for an already formed biofilm, reaching about 1 log inactivation [37]. Even with increased irradiance (138 μW/cm^2 in our case and 102 μW/cm^2 in [37]), there is no complete inactivation of the already formed biofilm, because of the protection offered by the extracellular polymeric substances. On the other hand, *P. aeruginosa* is known to produce a large amount of extracellular polymeric substances and is more resistant to UV-C irradiation than other bacteria, including

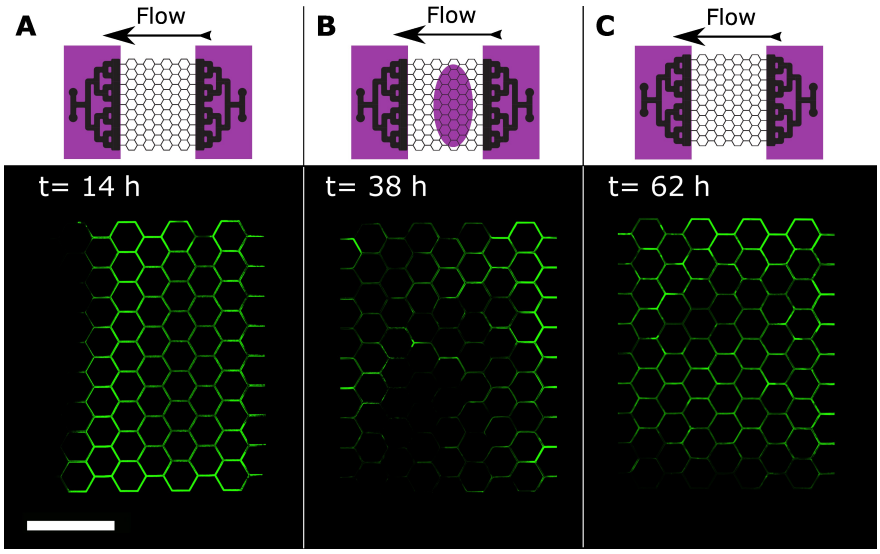

Figure 6 UV-C can be used to generate perturbations of a fully grown biofilm. **A.** Biofilm development 14 h after the inoculation, just before the start of the UV-C irradiation. **B.** State of the biofilm after 24 h of UV-C irradiation (38h after the inoculation). The drawing shows the area irradiated by the UV-C. At this moment, the UV-C led was just turned off. **C.** Recolonization of the biofilm 24 h after UV-C removal. The experiment was performed at 30°C at 2 μL/min. Scale bar 5 mm.

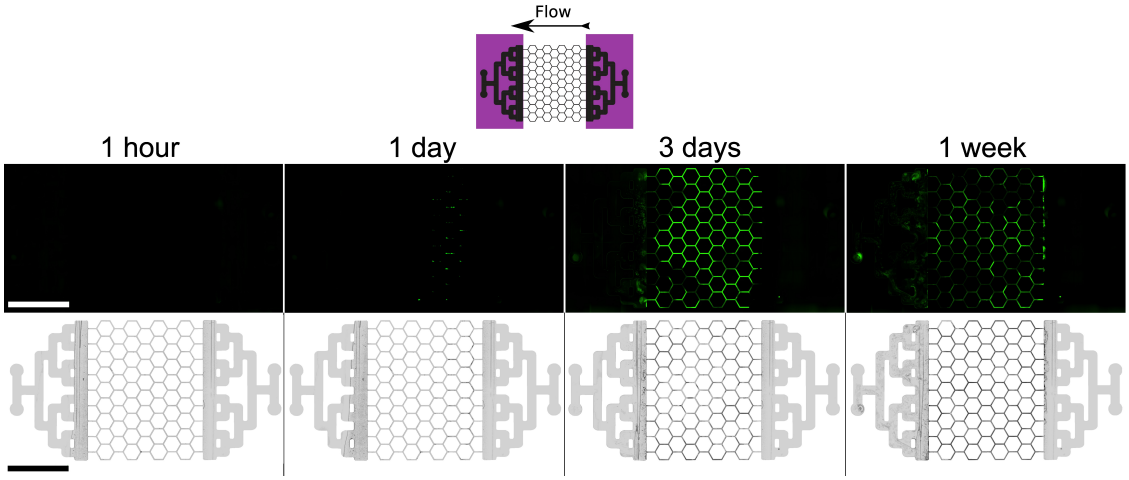

Figure 7 UV-C irradiation allows week-long experiments. Fluorescent images are on the top and bright field images on the bottom. We see that bacteria grow within the zone of interest but the inlet remains clean even after one week of growth. The outlet shows a limited number of biofilm patches due to detachments within the network and transport by the flow, but their growth is controlled by the UV-C light (see also supplementary material and Movie 2). The experiment was performed at 30°C and 2 μL/min. Scale bar 5 mm.

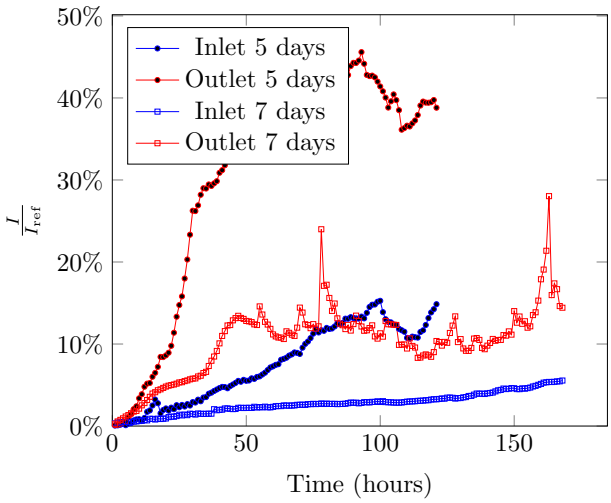

Figure 8 Relative intensity of GFP fluorescence for the inlet and outlet mixing zones during 5 and 7 days. The intensity (I) is expressed as a percentage of the maximum fluorescence integrated over the inlet mixing zone (I_{ref}) in the case without UV-C (Figs 2 and 3). The inlet shows a slow increase corresponding to the growth of the mushroom-like structures at the inlet of the hexagonal network. The inlet and outlet intensity in the case of 5 days increase faster due to a slight translation in the positioning of the UV-C system which allowed more colonization at the boundary with the hexagonal network. The outlet shows biomass attached in the mixing zones and fluctuations corresponding to detachment from the hexagonal network. The experiment was performed at 30°C and 2 μL/min (same as in Fig 7).

E. coli [40] for example. Since our approach does not require any integration directly to the chip, it can be used for a broad range of organisms and systems without costly changes to existing designs. If a higher level of control is required, one could increase the power of the UV-C illumination, for instance by increasing the number of LEDs — of course, heat dissipation would have to be dealt with properly. The guiding optics for UV-C could also be improved to gain in efficacy and to provide a finer control of the exact positioning of the irradiated zone, the UV-C power delivered to the sample and the uniformity of intensity distribution. This would broaden the range of potential applications of this technology.

Supplementary Material

See supplementary material for more details about experimental methods and effects of UV-C on growing biofilm.

Conflicts of interest

There are no conflicts to declare.

Acknowledgements

This work is part of a project that has received funding from the European Research Council (ERC) under the European Union's Horizon 2020 research and innovation programme (grant agreement No 803074). The authors thank Julien Lefort and Emmanuel Libert for their contribution to the design and fabrication of the UV-C system and Christophe Coudret for fruitful discussions. Photolithography for the mold fabrication has been done at LAAS-CNRS (UPR8001).

Notes and references

[1] Hans-Curt Flemming, Jost Wingender, Ulrich Szewzyk, Peter Steinberg, Scott A. Rice, and Staffan Kjelleberg. Biofilms: an emergent form of bacterial life. *Nature Reviews Microbiology*, 14(9):563–575, September 2016. Number: 9 Publisher: Nature Publishing Group. 1

[2] Alexander L. M. Chun, Ali Mosayyebi, Arthur Butt, Dario Carugo, and Maria Salta. Early biofilm and streamer formation is mediated by wall shear stress and surface wettability: A multifactorial microfluidic study. *MicrobiologyOpen*, 11(4):e1310, 2022. 1

[3] V. Gordon, M. Davis-Fields, K. Kovach, and C. Rodesney. Biofilms and mechanics: a review of experimental techniques and findings. *J. Phys. D: Appl. Phys.*, 50(22), 2017. 1

[4] Carey D. Nadell, Joao B. Xavier, and Kevin R. Foster. The sociobiology of biofilms. *FEMS Microbiology Reviews*, 33(1):206–224, January 2009. 1

[5] Giovanni Savorana, Jonasz Słomka, Roman Stocker, Roberto Rusconi, and Eleonora Secchi. A microfluidic platform for characterizing the structure and rheology of biofilm streamers. *Soft Matter*, 18(20):3878–3890, 2022. Publisher: Royal Society of Chemistry. 1

[6] Hans-Curt Flemming and Stefan Wuertz. Bacteria and archaea on Earth and their abundance in biofilms. *Nature Reviews Microbiology*, 17(4):247–260, April 2019. Number: 4 Publisher: Nature Publishing Group. 1

[7] Y. Bar-On, R. Phillips, and R. Milo. The biomass distribution on Earth. *PNAS*, 115(25), 2017. 1

[8] Mohammad Pousti, Mir Pouyan Zarabadi, Mehran Abbaszadeh Amirdehi, François Paquet-Mercier, and Jesse Greener. Microfluidic bioanalytical flow cells for biofilm studies: a review. *Analyst*, 144(1):68–86, December 2018. Publisher: The Royal Society of Chemistry. 1

[9] Luanne Hall-Stoodley, Paul Stoodley, Sandeep Kathju, Niels Høiby, Claus Moser, J. William Costerton, Annette Moter, and Thomas Bjarnsholt. Towards diagnostic guidelines for biofilm-associated infections. *FEMS Immunology & Medical Microbiology*, 65(2):127–145, July 2012. 1

[10] Sowmya Subramanian, Ryan C. Huiszoon, Sangwook Chu, William E. Bentley, and Reza Ghodssi. Microsystems for biofilm characterization and sensing – A review. *Biofilm*, 2:100015, December 2020. 1

[11] Nicholas B Justice, Chongle Pan, Ryan Mueller, Susan E Spaulding, Vega Shah, Christine L Sun, Alexis P Yelton, Christopher S Miller, Brian C Thomas, Manesh Shah, Nathan VerBerkmoes, Robert Hettich, and Jillian F Banfield. Heterotrophic archaea contribute to carbon cycling in low-ph, suboxic biofilm communities. *Appl Environ Microbiol*, 78(23):8321–8330, sep 2012. 1

[12] Di Wang, Anming Xu, Claudine Elmerich, and Luyan Z. Ma. Biofilm formation enables free-living nitrogen-fixing rhizobacteria to fix nitrogen under aerobic conditions. *The ISME Journal*, 11(7):1602–1613, Jul 2017. 1

[13] Anurag Maurya, Manoj Kumar Singh, and Sushil Kumar. Biofiltration technique for removal of waterborne pathogens. pages 123–141, 2020. 1

[14] Sandhya Mishra, Yaohua Huang, Jiayi Li, Xiaozhen Wu, Zhe Zhou, Qiqi Lei, Pankaj Bhatt, and Shaohua Chen. Biofilm-mediated bioremediation is a powerful tool for the removal of environmental pollutants. *Chemosphere*, 294:133609, January 2022. 1

[15] C. Nadell, K. Drescher, and K. Foster. Spatial structure, cooperation and competition in biofilms. *Nature Reviews Microbiology*, 14:589–600, 2016. 1

[16] Julian Wimpenny, Werner Manz, and Ulrich Szewzyk. Heterogeneity in biofilms. *FEMS Microbiology Reviews*, 24(5):661–671, December 2000. 1

[17] Jurrien M. Vroom, Kees J. De Grauw, Hans C. Gerritsen, David J. Bradshaw, Philip D. Marsh, G. Keith Watson, John J. Birmingham, and Clive Allison. Depth penetration and detection of pH gradients in biofilms by two-photon excitation microscopy. *Applied and Environmental Microbiology*, 65(8):3502–3511, August 1999. 1

[18] Alma Dal Co, Simon van Vliet, and Martin Ackermann. Emergent microscale gradients give rise to metabolic cross-feeding and antibiotic tolerance in clonal bacterial populations. *Philosophical Transactions of the Royal Society B: Biological Sciences*, 374(1786):20190080, October 2019. 1

[19] Alexander D. Klementiev, Zhaoyu Jin, and Marvin Whiteley. Micron scale spatial measurement of the o2 gradient surrounding a bacterial biofilm in real time. *mBio*, 11(5), October 2020. 1

[20] Yutaka Yawata, Jen Nguyen, Roman Stocker, and Roberto Rusconi. Microfluidic Studies of Biofilm Formation in Dynamic Environments. *Journal of Bacteriology*, 198(19):2589–2595, October 2016. 1

[21] Whitesides GM Weibel DB, Diluzio WR. Microfabrication meets microbiology. *Nature Reviews Microbiology*, 5(3):209–218, 2007. 1

[22] Kiran Raj M and Suman Chakraborty. PDMS microfluidics: A mini review. *Journal of Applied Polymer Science*, 137(27):48958, January 2020. 1

[23] Adam P. Vollmer, Ronald F. Probstein, Richard Gilbert, and Todd Thorsen. Development of an integrated microfluidic platform for dynamic oxygen sensing and delivery in a flowing medium. *Lab on a Chip*, 5(10):1059, 2005. 1

[24] Inês Miranda, Andrews Souza, Paulo Sousa, João Ribeiro, Elisabete M. S. Castanheira, Rui Lima, and Graça Minas. Properties and applications of PDMS for biomedical engineering: A review. *Journal of Functional Biomaterials*, 13(1):2, December 2021. 1

[25] Stocker R Rusconi R, Garren M. Microfluidics expanding the frontiers of microbial ecology. *Annual Review of Biophysics*, 43:65–91, 2014. 1

[26] Tanvir Ahmed, Thomas S. Shimizu, and Roman Stocker. Microfluidics for bacterial chemotaxis. *Integrative Biology*, 2(11–12):604–629, 2010. 1

[27] MK Kim, F Ingremeau, A Zhao, BL Bassler, and HA Stone. Local and global consequences of flow on bacterial quorum sensing. *Nature Microbiology*, 1:15005, 2016. 1

[28] Felix J. H. Hol and Cees Dekker. Zooming in to see the bigger picture: Microfluidic and nanofabrication tools to study bacteria. *Science*, 346(6208):1251821, 2014. 1

[29] Jayde A. Aufrecht, Jason D. Fowlkes, Amber N. Bible, Jennifer Morrell-Falvey, Mitchel J. Doktycz, and Scott T. Retterer. Pore-scale hydrodynamics influence the spatial evolution of bacterial biofilms in a microfluidic porous network. *PLOS ONE*, 14(6):1–17, 06 2019. 1

[30] Katharine Z. Coyte, Hervé Tabuteau, Eamonn A. Gaffney, Kevin R. Foster, and William M. Durham. Microbial competition in porous environments can select against rapid biofilm growth. *Proceedings of the National Academy of Sciences*, 114(2):E161–E170, January 2017. Publisher: Proceedings of the National Academy of Sciences. 1

[31] Yutaka Yawata, Otto X. Cordero, Filippo Menolascina, Jan-Hendrik Hehemann, Martin F. Polz, and Roman Stocker. Competition–dispersal tradeoff ecologically differentiates recently speciated marine bacterioplankton populations. *Proceedings of the National Academy of Sciences*, 111(15):5622–5627, 2014. 1

[32] Lei Yang, Janus A. J. Haagensen, Lars Jelsbak, Helle Krogh Johansen, Claus Sternberg, Niels Høiby, and Søren Molin. In situ growth rates and biofilm development of pseudomonas aeruginosa populations in chronic lung infections. *Journal of Bacteriology*, 190(8):2767–2776, April 2008. 2.4

[33] Johannes Schindelin, Ignacio Arganda-Carreras, Erwin Frise, Verena Kaynig, Mark Longair, Tobias Pietzsch, Stephan Preibisch, Curtis Rueden, Stephan Saalfeld, Benjamin Schmid, Jean-Yves Tinevez, Daniel James White, Volker Hartenstein, Kevin Eliceiri, Pavel Tomancak, and Albert Cardona. Fiji: an open-source platform for biological-image analysis. *Nature Methods*, 9(7):676–682, June 2012. 2.7

[34] R.V. Pereira, M.L. Bicalho, V.S. Machado, S. Lima, A.G. Teixeira, L.D. Warnick, and R.C. Bicalho. Evaluation of the effects of ultraviolet light on bacterial contaminants inoculated into whole milk and colostrum, and on colostrum immunoglobulin g. *Journal of Dairy Science*, 97(5):2866–2875, May 2014. 3.1, 4

[35] Carla C. C. R. de Carvalho. Biofilms: Microbial strategies for surviving UV exposure. In *Advances in Experimental Medicine and Biology*, pages 233–239. Springer International Publishing, 2017. 3.1

[36] Mohamed O. Elasri and Robert V. Miller. Study of the response of a biofilm bacterial community to UV radiation. *Applied and Environmental Microbiology*, 65(5):2025–2031, May 1999. 3.1

[37] Hamed Torkzadeh and Ezra L. Cates. Biofilm growth under continuous UVC irradiation: Quantitative effects of growth conditions and growth time on intensity response parameters. *Water Research*, 206:117747, November 2021. 4

[38] Stephanie L. Gora, Kyle D. Rauch, C. Carolina Ontiveros, Amina K. Stoddart, and Graham A. Gagnon. Inactivation of biofilm-bound Pseudomonas aeruginosa bacteria using UVC light emitting diodes (UVC LEDs). *Water Research*, 151:193–202, March 2019. 4

[39] Ben Ma, Saba Seyedi, Emma Wells, David McCarthy, Nicholas Crosbie, and Karl G. Linden. Inactivation of biofilm-bound bacterial cells using irradiation across UVC wavelengths. *Water Research*, 217:118379, June 2022. 4

[40] Surapong Rattanakul and Kumiko Oguma. Inactivation kinetics and efficiencies of UV-LEDs against pseudomonas aeruginosa, legionella pneumophila, and surrogate microorganisms. *Water Research*, 130:31–37, March 2018. 4